

Research article

WDR5, ASH2L, AND RBBP5 CONTROL THE EFFICIENCY OF *FOS* TRANSCRIPT PROCESSING

PEIK LIN TEOH^{1,2,*} and ANDREW D. SHARROCKS²

¹Biotechnology Research Institute, Universiti Malaysia Sabah, Jalan UMS, 88400 Kota Kinabalu, Sabah, Malaysia, ²Faculty of Life Sciences, University of Manchester, Michael Smith Building, Oxford Road, Manchester, M13 9PT, U.K.

Abstract: H3K4 trimethylation is strongly associated with active transcription. The deposition of this mark is catalyzed by SET-domain methyltransferases, which consist of a subcomplex containing WDR5, ASH2L, and RBBP5 (the WAR subcomplex); a catalytic SET-domain protein; and additional complex-specific subunits. The ERK MAPK pathway also plays an important role in gene regulation via phosphorylation of transcription factors, co-regulators, or histone modifier complexes. However, the potential interactions between these two pathways remain largely unexplored. We investigated their potential interplay in terms of the regulation of the immediate early gene (IEG) regulatory network. We found that depletion of components of the WAR subcomplex led to increased levels of unspliced transcripts of IEGs that did not necessarily reflect changes in their mature transcripts. This occurs in a manner independent from changes in the H3K4me3 levels at the promoter region. We focused on *FOS* and found that the depletion of WAR subcomplex components affected the efficiency of *FOS* transcript processing. Our findings show a new aspect of WAR subcomplex function in coordinating active transcription with efficient pre-mRNA processing.

* Author for correspondence. Email: peiklin@ums.edu.my, phone: +6088-320000 ext. 8471, fax: +6088-320993

Abbreviations used: ChIP – chromatin immunoprecipitation; EGF – epidermal growth factor; ERK – extracellular signal-regulated kinases; FBS – fetal bovine serum; H3K4 – histone 3 lysine 4; H3K4me3 – trimethylation of histone 3 lysine 4; HAT – histone acetyltransferase; HDAC – histone deacetylase; HMT – histone methyltransferases; IEG – immediate early genes; MAPK – mitogen-activated protein kinase; MLL – mixed-lineage leukemia; NRO – nuclear run on; PAGE – polyacrylamide gel electrophoresis; PBS – phosphate-buffered saline; Pol II – RNA polymerase II; SDS – sodium dodecyl sulphate; RNAi – RNA interference; siRNA – small interfering RNA; WAR – WDR5–ASH2L–RBBP5

Keywords: RBBP5, ASH2L, WDR5, Histone methyltransferase, Immediate early gene, Splicing

INTRODUCTION

Several histone 3 lysine 4 methyltransferases have been identified in mammals: SETD1A, SETD1B, MLL1, MLL2, MLL3, and MLL4 [1–3]. All of these are capable of methylating histone H3 at lysine residue 4. The complexity of MLL/SET histone methyltransferases (HMTs) in mammals indicates that H3K4 methylation is functionally important and non-redundant in higher eukaryotes, whereas yeast only has one H3K4 methylase complex, COMPASS, which is capable of mono-, di- and trimethylation of histone H3.

The six catalytic subunits of the H3K4 HMTs share a conserved SET domain that is responsible for their catalytic activity, but their other domains are dissimilar. SET/MLLs gain their full HMT activity by interacting with core component proteins such as WDR5, ASH2L, and RBBP5 [4–9]. This core subunit is called the WAR (WDR5, ASH2L, and RBBP5) subcomplex in our study, although DPY30 has recently been demonstrated to be associated with it [7].

Other complexes have their own unique subunits. For example, WDR82 is only found in SETD1A/1B complexes, while MENIN is only present in MLL1/2 [1, 8]. The WAR subcomplex has been shown to enhance the activity of the catalytic domain of associated methyltransferases [9, 10]. In addition to the commonly associated SET domain-containing proteins, the WRAD (WDR5, RBBP5, ASH2L, and DPY30) complex was recently categorized as a novel non-SET domain methyltransferase [7]. Furthermore, heterodimers of ASH2L and RBBP5 have been shown to possess methyltransferase activity in vitro, recognizing its substrates via the SPRY domain found in ASH2L [11]. However, the intrinsic H3K4 methylating activities of both WRAD and the ASH2L/RBBP5 heterodimer are weak when using a histone H3 tail peptide as a substrate [7, 11]. Recombinant WRAD proteins were also found to form an independent complex without an associated SET domain [7, 12, 13].

Importantly, previous studies showed that RBBP5 is overexpressed in glioblastoma patients [14] and that the expression of ASH2L protein is increased in most human cancers [15]. These findings suggest that the components of the H3K4 HMT complex might have alternative roles independent of SET domain proteins.

H3K4 trimethylation is predominantly associated with active transcription based on genome-wide analysis of its occupancy at transcription start sites. There are multiple enzymes involved in depositing this mark across the genome, but the mechanism of its deposition is elusive. Studies have shown that SETD1-mediated methylation is more widespread as depletion of SETD1 protein causes a global loss of this mark [16], while H3K4 methylation mediated by MLL1/2 methyltransferases is more gene-specific [17].

In addition to gene activation, histone methylation also participates in other biological functions. Many studies on MLLs are based on their roles in the

activation of *HOX* genes [17, 18]. Recently, their roles as co-regulators in nuclear receptor-mediated gene activation and hormone signaling have begun to emerge. Interactions of MLLs with nuclear receptors, such as retinoic acid receptors, liver X receptors, and estrogen receptors, have been widely studied [19]. It has also been shown that the promoters of inducible genes are enriched with the H3K4me3 mark, but how this modification contributes to gene induction remains largely unexplored. The presence of this mark is suggested to be important for the rapid induction of gene transcription.

Interestingly, recent studies have shown that during immediate early gene (IEG) induction, the accumulation of full-length and incompletely spliced transcripts of IEGs occurs in the nucleus, and that there is little evidence of co-transcriptional splicing for IEGs [20]. In addition, H3K4 trimethylation has been linked to transcription and pre-mRNA processing by bridging spliceosomal components to this mark through the recruitment of CHD1 [21].

The Ras/ERK MAP kinase pathway plays an important role in many physiological processes and is often upregulated in human cancers [22]. Molecularly, one major function of this pathway is to activate the expression of IEGs like *FOS* [23, 24]. In the case of *FOS*, ERK directly phosphorylates the transcription factor ELK1, which binds to its promoter region and ultimately promotes transcriptional initiation and elongation. However, while nucleosomes in the vicinity of the *FOS* promoter are subjected to several dynamic modifications, they also show high levels of H3K4 trimethylation, which remains at a constant level [25]. It is therefore unclear what role H3K4 trimethylation might play in the induction of IEGs such as *FOS*. However, H3K4me3 has been shown to be associated with pre-mRNA maturation of other IEGs, such as *FRA1* and *IRF1* [21].

An RNAi screen in *Caenorhabditis elegans* showed that the H3K4 methyltransferase set-16 attenuates Ras signaling [26], suggesting a possible genetic link between these two pathways. It is unknown whether this interaction is direct or indirect, but this link might also occur in mammals. Therefore, we aimed to probe the potential links between the Ras/ERK MAPK pathway and the H3K4 methyltransferase complex by studying the role of the WAR subcomplex in IEG induction following Ras/ERK MAPK pathway activation. In this study, we uncovered a new function of the WAR subcomplex in regulating gene expression. We found that WAR complex depletion caused increases in the pre-mRNA levels of IEGs. By focusing on *FOS*, we showed that this increase is at least partially due to defects in transcript processing.

MATERIALS AND METHODS

Cell culture and transfections

The human cervical cancer cell line HeLa S3 was maintained in Dulbecco's modified Eagle's medium (DMEM) supplemented with 10% fetal bovine serum (FBS). Cell lines were incubated at 37°C with 5% CO₂.

SMARTpool siRNA duplexes against *GAPDH*, *RBBP5*, *ASH2L*, and *WDR5* were obtained from Dharmacon. RNA interference was performed using Lipofectamine 2000 (Invitrogen) according to the manufacturer's instructions. For RNA extraction, 1.1×10^5 cells in 12-well plates were transfected with 0.5 μ l of 20 μ M siRNA and 2 μ l of lipofectamine. For ChIP experiments, 1×10^6 cells were transfected with 9 μ l of 20 μ M siRNA and 36 μ l of lipofectamine in 10-cm plates. Where indicated, cells were serum-starved for 24 h then treated with 300 ng/ml of epidermal growth factor (EGF).

RNA extraction and RT-PCR

Total RNA was extracted using an RNeasy kit (Qiagen) according to the manufacturer's protocol. RT-PCR was carried out as previously described [27]. Data were analyzed using the Rotor-Gene 6 software (Qiagen). The following primers were used:

- *FOS*, ADS4029 (AGAATCCGAAGGGAAAGGAA) and ADS4030 (CTTCTCCTTCAGCAGGTTGG);
- *ZFP36*, ADS3964 (ATCCGACCCTGATGAATATG), and ADS3963 (AGAGATGCGATTGAAGATGG);
- *ACTB*, ADS3962 (CCCAGCACAATGAAGATCAA), and ADS3961 (CACCTTCACCGTTCCAGTTT);
- *PreFOS*, ADS3934 (ACCCGCAGACTCCTTCTCCA), and ADS3933 (GTGCGTGCGCTCAGAGCAA);
- *PreZFP36*, ADS3932 (GAGCCCACAAACCGGCCT), and ADS3931 (AGTCCCTCCATGGTCGGATG);
- *PreACTB*, ADS3930 (ACATTAAGGAGAAGCTGTGCT), and ADS3929 (GTAACCCTCATGTCAGGCA);
- *18S*, ADS4005 (CGGCTACCACATCCAAGGAA), and ADS4006 (GCTGGAATTACCGCGGCT).

Chromatin immunoprecipitation (ChIP)

ChIP assays were carried out as described previously [28] using rabbit anti-H3K4me3 (Millipore), rabbit anti-Histone H3 (Abcam), and rabbit anti-IgG (Upstate). Briefly, cells were cross-linked with 1% formaldehyde for 10 min at room temperature, harvested, and rinsed with $1 \times$ DPBS. Cell nuclei were isolated, pelleted, and sonicated. DNA fragments were enriched using beads that were pre-bound with the respective antibody. After reversing the cross-links, the enriched DNA was purified and analyzed via real-time PCR. The following primer pairs were used:

- *FOS* promoter (-353/-185), ADS1676 (5'-GAGCAGTTCCCGTCAATCC-3'), and ADS1677 (5'-GCATTTTCGAGTTCTGTCT-3');
- *FOS* negative region (-3395/-3209), ADS1688 (5'-CAGATCTGCAAATGGCAAAA-3'), and ADS1689 (5'-TCTCCTGCCCACTAACATC-3');
- *ZFP36* promoter (-350/-520), ADS3905 (5'-CCCCATCGGGCTTCTGCT-3'), and ADS3905 (5'-GTGGACAGCCGTGACCGA-3');

- *RPL41* promoter (+195/+264), ADS3913 (5'-CGCCATGAGAGCCAAGGT-3'), and ADS3912 (5'-TCGCTACTACTCGCCAACCTCCTA-3').

Western blot analysis

Western blotting was performed using the following primary antibodies; rabbit anti-RBBP5 (Bethyl), rabbit anti-H3K4me3 (Millipore), mouse anti-phospho-ERK1/2 (Cell Signalling), and rabbit anti-ERK2 (Santa Cruz Biotechnology). The proteins were detected via chemiluminescence with SuperSignal West Dura Substrate (Thermo Scientific) and visualized with a Fluoro-S MultiImager (Bio-Rad).

RESULTS

The role of the WAR subcomplex in determining the spliced and unspliced RNA levels of IEGs

To study the interaction between the WAR subcomplex and the Ras/ERK pathway, we first attempted to identify potential common target genes. We compared gene expression data generated in EGF-treated HeLa cells [29] and RBBP5 ChIP-chip data from the same cell type [30]. We identified 118 genes that were found to be upregulated 1.5-fold by EGF treatment and to also be bound by RBBP5 (supplementary material at <http://dx.doi.org/10.2478/s11658-014-0190-8>). Amongst these genes were the IEGs, *FOS*, and *ZFP36*. We verified the binding of RBBP5 to their promoter regions (Fig. 1).

Importantly, the magnitude of binding to the *FOS* and *ZFP36* promoters was of a similar magnitude to the positive controls, *HOXC9* and *RPL41*, which also showed RBBP5 occupancy in their promoter regions, as expected [31]. RBBP5 occupancy at all the promoter regions was reduced after depletion, further demonstrating the specificity of the ChIP signal. RBBP5 binding following RBBP5 depletion at both the *FOS* and *ZFP36* promoters was consistently reduced in three independent experiments, ranging between 0.5- and 0.7-fold reductions on the *FOS* promoter and 0.3- to 0.8-fold reductions on the *ZFP36* promoter. This is clear evidence for RBBP5 binding to the *FOS* and *ZFP36* promoters.

Having established RBBP5 occupancy, we then asked how RBBP5 and other components of the WAR subcomplex might affect ERK pathway-mediated expression of *FOS* and *ZFP36*. Members of the WAR subcomplex were individually depleted in HeLa cells, and cells were then serum-starved and then treated with EGF to activate the ERK pathway. The effectiveness of siRNA silencing was determined at the protein (Fig. 2A) and RNA levels (Fig. 2B). Substantial reductions in both the protein and RNA levels of RBBP5, *ASH2L*, and *WDR5* were observed after respective siRNA silencing (Fig. 2), with over 90% reduction in *RBBP5*, *ASH2L*, and *WDR5* transcript levels after siRNA-mediated depletion (Fig. 2B). The siRNA-mediated depletion was specific: little evidence of cross-regulation of other WAR subcomplex components was seen.

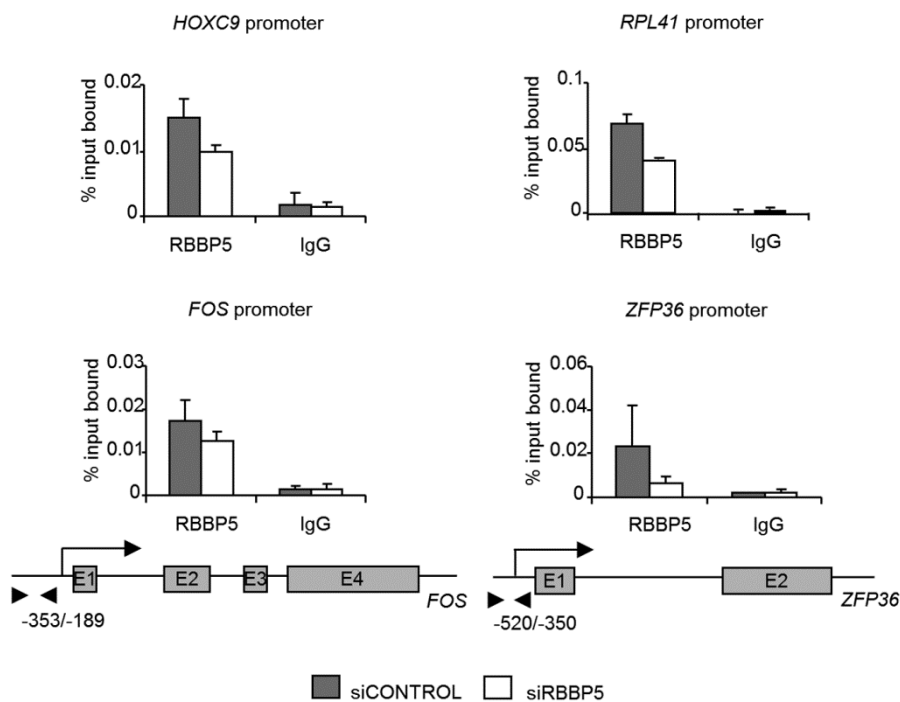


Fig. 1. RBBP5 is recruited to the *FOS* and *ZFP36* promoters. HeLa S3 cells were transfected with siRNA against *GAPDH* (siControl) or *RBBP5* for 48 h. Sonicated nuclear lysates were used for ChIP using α -RBBP5 or α -IgG antibodies. qPCR-ChIP analysis of RBBP5 occupancy was performed at positive controls (*HOXC9* and *RPL41* promoters) and the *FOS* and *ZFP36* promoters. Schematic diagrams representing the locations of the primer pairs (inverted arrowheads) used to amplify the IEG promoters are shown. Exons are indicated as E1–E4 in the boxes. Data are shown as the percentage of input bound by each antibody. Error bars represent standard deviations calculated from three biologically independent samples. Each sample for qPCR was performed with 2 replicates.

Next, to probe a potential role in transcriptional activation we investigated the effect of WAR subcomplex depletion on the expression of newly synthesized nascent pre-mRNA from the IEGs, *FOS* and *ZFP36*. In cells treated with control siRNA, EGF treatment caused a transient increase in the transcription of *FOS* with a maximal increase of unspliced transcripts at 15 min followed by a gradual decrease as EGF treatment was prolonged to 1 h. However, upon depletion of RBBP5, a significant increase (twofold) of unspliced *FOS* RNA was observed at 15 min after EGF treatment (Fig. 3B, left panel). However, this increase was not observed at other times.

We then assessed whether this phenomenon would also be seen in WDR5- and ASH2L-depleted cells. Upon WDR5 and ASH2L silencing, similar increases in unspliced transcript levels were observed for *FOS* after 15 min of EGF stimulation as we demonstrated upon RBBP5 knockdown (Fig. 3B, middle and

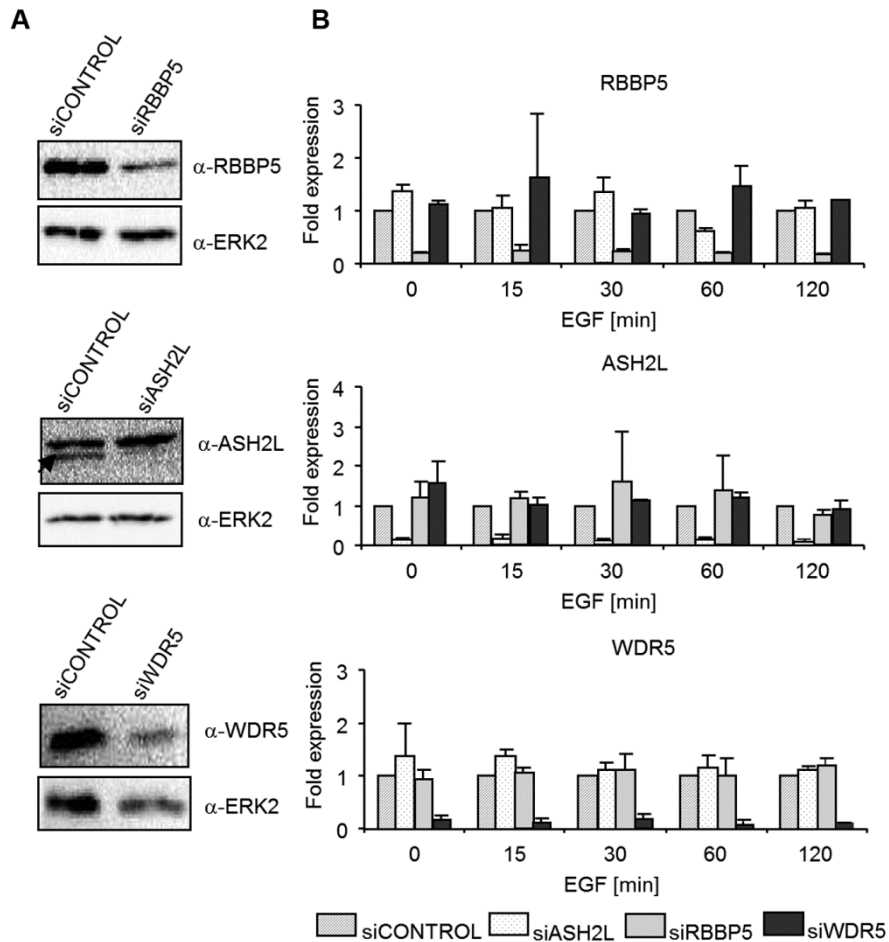


Fig. 2. Validation of the effectiveness of siRNA silencing. A – HeLa S3 cells were transfected with siRNA against *GAPDH* (siControl), *RBBP5*, *ASH2L*, and *WDR5* for 48 h. The protein levels of RBBP5, ASH2L, and WDR5 were determined after siRNA silencing by western blotting using the indicated antibodies. Anti-ERK2 antibody was used as a loading control. The efficiency of knockdown at the protein level was typically a 30–50% reduction in RBBP5 protein levels and a 20–70% reduction in WDR5 protein levels following siRNA treatment. B – The mRNA expression levels of *RBBP5*, *ASH2L*, and *WDR5*. HeLa S3 cells were prepared as described in (A) but with or without EGF treatment for the times indicated. RNA was extracted and qRT-PCR analysis of the indicated genes was performed. Error bars represent standard deviations calculated from three biologically independent samples. Each knockdown sample was normalized to the RNA level in cells containing control siRNA at the corresponding times (taken as 1).

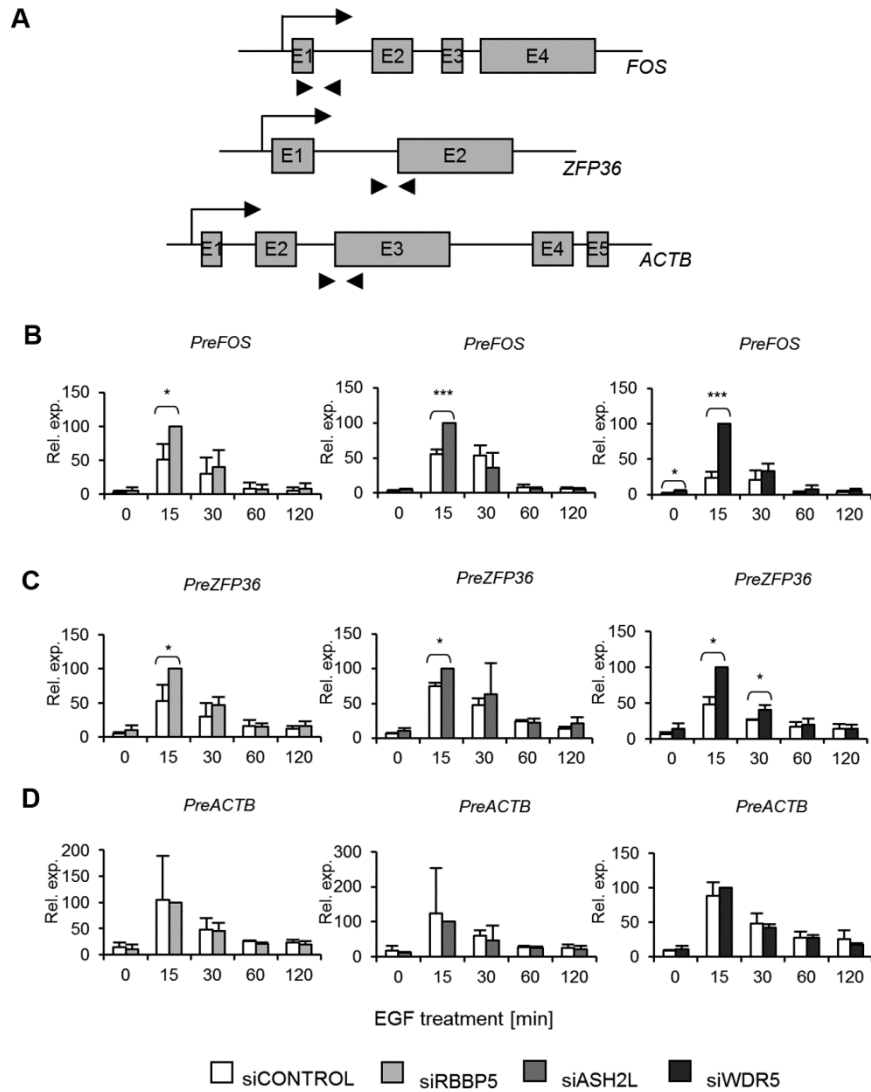


Fig. 3. The role of the WAR subcomplex components in determining pre-mRNA levels of immediate early genes. A – Schematic diagram showing the locations of the primer pairs (inverted arrowheads) used to amplify the indicated gene loci. Exons are indicated as E1–E5 in the boxes. B through D – HeLa S3 cells were transfected with siRNA against *GAPDH* (siControl), *RBBP5*, *ASH2L*, or *WDR5* and serum-starved. After 48 h, cells were treated with EGF for the indicated times. RNA was extracted and qRT-PCR analysis was performed for the indicated genes using primers targeting the pre-mRNA of (B) *FOS*, (C) *ZFP36*, and (D) *ACTB*. The relative expression was obtained after normalization to 18S RNA and further normalized to their expression in the presence of each specific siRNA duplex at 15 min (taken as 100). Error bars represent standard deviations calculated from three biologically independent samples. Asterisks denote differences with statistical significances: * $p < 0.05$, ** $p < 0.005$ and *** $p < 0.0005$ (obtained from a 2-tailed *t* test).

right panels). Similar to *FOS*, we also observed concomitant increases in unspliced transcript levels for *ZFP36* after *RBBP5*, *ASH2L* and *WDR5* silencing in EGF-treated cells after 15 min (Fig. 3C). Although we saw an increase in the unspliced transcript level for the control gene *ACTB* in EGF-treated cells, there was no change in its expression level after depletion of the WAR complex components (Fig. 3D). This indicates that the increase in unspliced transcript levels observed for IEGs is a specific event, as the transcription of the *ACTB* gene is not altered upon depletion of the WAR complex components.

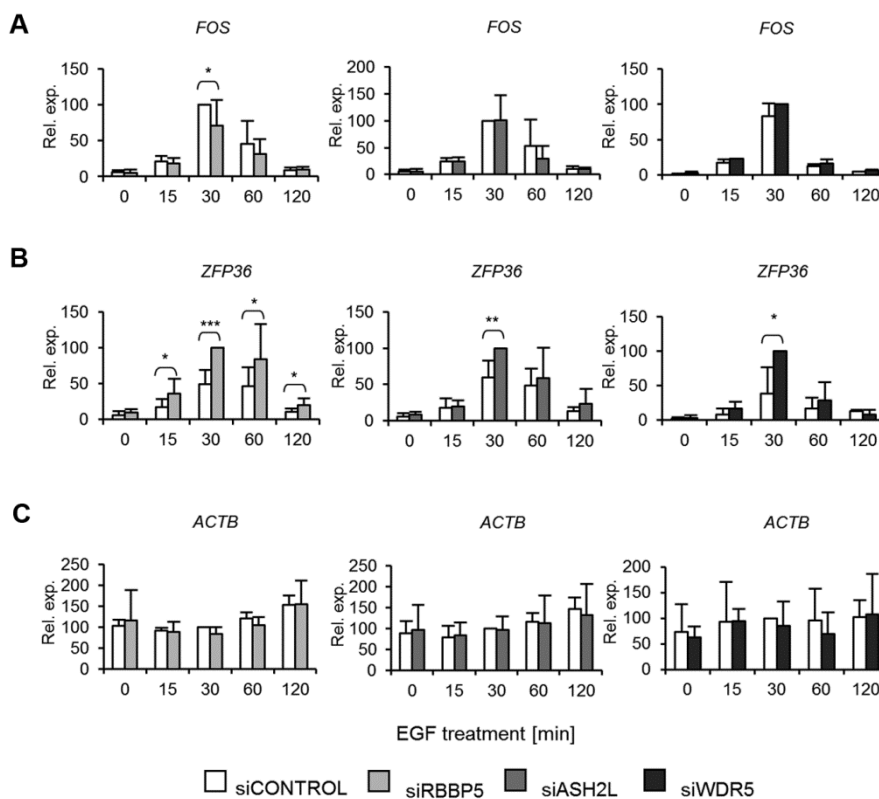


Fig. 4. The role of WAR subcomplex components in controlling mature mRNA levels of immediate early genes. HeLa S3 cells were transfected with siRNA against *GAPDH* (siControl), *RBBP5*, *ASH2L*, or *WDR5* and serum-starved. After 48 h, cells were treated with EGF as indicated. RNA was extracted and qRT-PCR analysis of the indicated genes was performed using primers targeting the mRNA of (A) *FOS*, (B) *ZFP36*, and (C) *ACTB*. The relative expressions were obtained after normalization to 18S RNA and further normalized to their expression in the presence of either each specific siRNA duplex or the control siRNA (whichever was the higher) at 30 min (taken as 100). Error bars represent standard deviations calculated from seven, eight, and three biologically independent samples of siRBBP5, siASH2L, and siWDR5, respectively. Asterisks denote differences with statistical significances: * $p < 0.05$, ** $p < 0.005$ and *** $p < 0.0005$ (obtained from a 2-tailed *t* test).

Next, we asked whether the increases in unspliced transcript levels caused by WAR complex depletion translated into increases in mature mRNA levels. As expected, EGF treatment caused a rapid increase in *FOS* and *ZFP36* levels, with peak levels at 30 min (Fig. 4A and 4B). This timing is consistent with the delay required for the splicing of pre-mRNAs, which increase maximally after 15 min. Surprisingly, our results demonstrated that RBBP5 depletion did not cause increases in the mRNA levels of *FOS*. If anything, it resulted in reductions in mRNA levels (Fig. 4A). Similarly, no increases in spliced *FOS* transcript levels were observed in WDR5- or ASH2L-depleted cells (Fig. 4A, middle and right panels). By contrast, mature, spliced *ZFP36* transcripts were significantly increased in EGF-treated cells at 30 min after individually depleting each of the WAR complex components (Fig. 4B). Depletion of the WAR complex components did not affect the mRNA levels of the control gene, *ACTB* (Fig. 4C). These results demonstrate that depletion of the WAR subcomplex leads to increases in the unspliced transcripts of both *FOS* and *ZFP36*. Only in the case of *ZFP36* is this increase converted to an increase in mature mRNA levels.

The processing of *FOS* mRNA is affected by depletion of WAR complex components

Next, we investigated whether the WAR subcomplex is involved in controlling post-transcriptional processes. One potential point of control is in RNA processing and in particular RNA splicing. We focused on *FOS*, as the increase in unspliced transcripts in *FOS* was not reflected in its spliced transcript levels upon WAR complex depletion. To investigate whether splicing events were potentially compromised through perturbations in the WAR subcomplex, we monitored the ratio of pre-mRNA to mRNA in the same RNA samples as an indicator of splicing efficiency. An increase in the pre-mRNA/mRNA ratio would indicate that a decrease in splicing occurs (or vice versa).

The results showed that the rate of splicing of *FOS* was slowest 15 min after EGF induction compared to the later times, suggesting that splicing rates are unable to keep up with the enhanced transcription rates at this time (Fig. 5A). The splicing efficiency is then increased after 30 min, leading to the production of maximal mature mRNA levels. However, upon RBBP5 depletion, we observed a threefold decrease in splicing efficiency of the *FOS* message compared to control cells after 15 min EGF treatment (Fig. 5A). This decrease in splicing efficiency was also observed in WDR5- and ASH2L-depleted cells although in the latter case this was not statistically significant (Fig. 5A, middle and right panels). By contrast, the splicing efficiency of the negative control gene, *ACTB*, was not significantly altered by depletion of any of the WAR complex components (Fig. 5B). These results are consistent with a role for the WAR subcomplex in modulating *FOS* transcript levels through controlling its splicing efficiency.

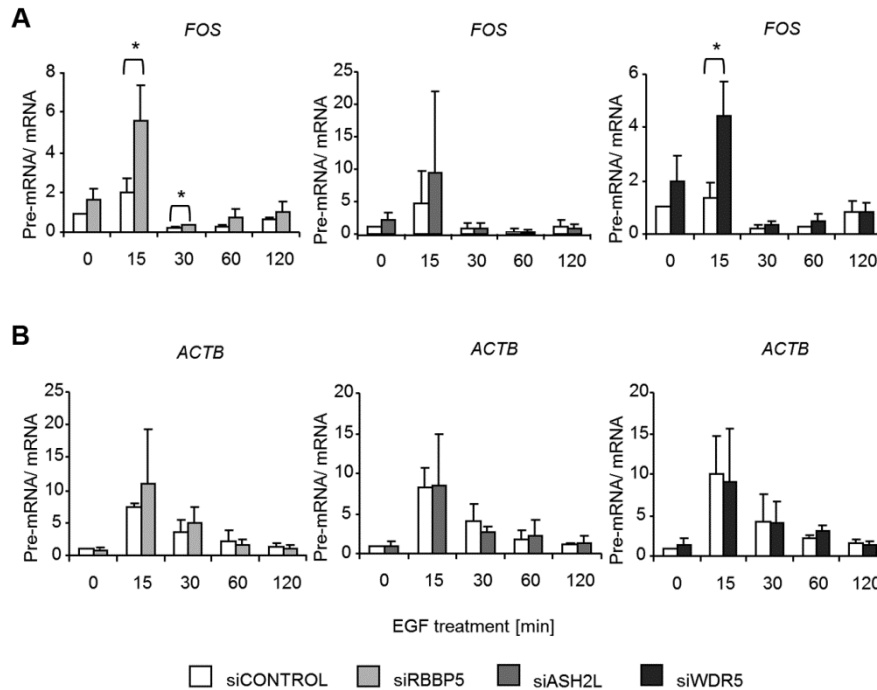


Fig. 5. The role of the WAR subcomplex components in the processing of *FOS* mRNA. HeLa S3 cells were transfected with siRNA against *GAPDH* (siControl), *RBBP5*, *ASH2L*, or *WDR5*. After 48 h, the serum-starved cells were treated with EGF for up to 2 h. RNA was extracted and qRT-PCR analysis of (A) *FOS* or (B) *ACTB* was performed using primers targeting mRNA or pre-mRNA. The mRNA or pre-mRNA levels of the indicated genes relative to 18S RNA were calculated and then the ratios of pre-mRNA to mRNA were normalized to siControl without treatment (taken as 1). The ratio of pre-mRNA to mRNA indicates the splicing efficiency. Error bars represent standard deviations calculated from three biologically independent samples. Asterisks denote differences with statistical significance: * $p < 0.05$ (obtained from a 2-tailed t test).

Depletion of WAR subcomplex components does not affect H3K4 trimethylation levels at the *FOS* promoters

As the WAR subcomplex has previously been implicated in controlling H3K4me3 levels, it seemed likely that this was its mode of action. We therefore examined whether this was also the case at the *FOS* promoter, and whether this could therefore be linked to the RNA processing defects we observed. We used ChIP to investigate the effect of RBBP5 depletion on H3K4me3 levels at the *FOS* promoter. We solely focused on 15 min EGF treatment because the knockdown of WAR complex components caused significant increases in pre-mRNA level at that particular time.

First we confirmed that a reduction in global levels of H3K4me3 occurred upon RBBP5 silencing by western blotting (Fig. 6A, lanes 3 and 4). We also included

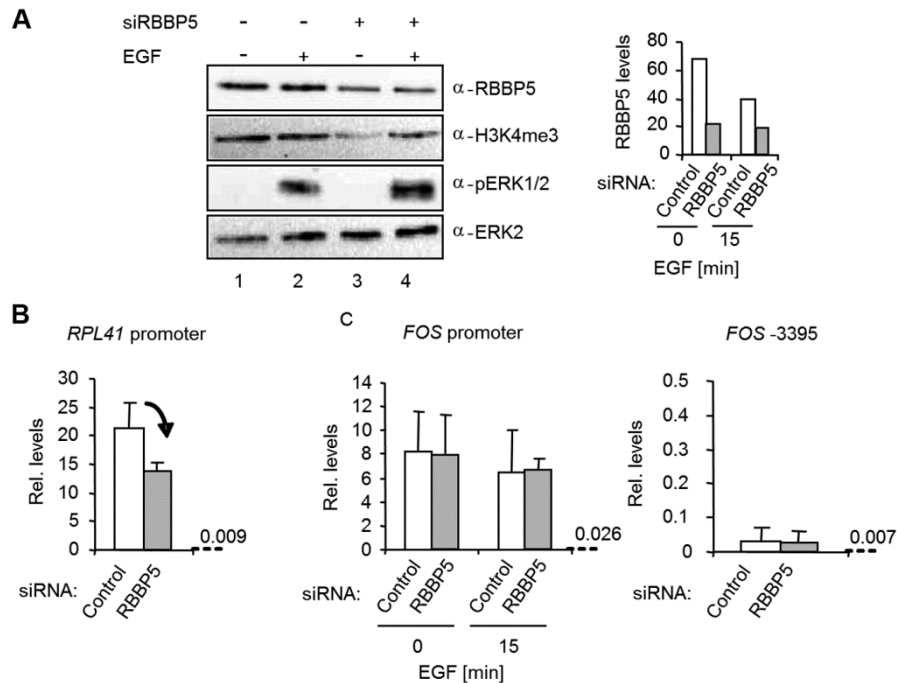


Fig. 6. RBBP5 depletion does not affect H3K4 trimethylation levels at the *FOS* promoter. HeLa S3 cells were transfected with siRNA against *GAPDH* (siControl) or *RBBP5* and serum-starved. After 48 h, cells were left untreated or treated with EGF for 15 min and lysates were used for western analysis or ChIP with α -H3K4me3, α -H3 or non-specific α -IgG antibodies. A – Sonicated nuclear lysates were analyzed by western blotting using the antibodies as indicated. ERK2 was used as a loading control. The results of quantitative analyses of RBBP5 knockdown efficiency are shown in the right panel. They were calculated by normalizing RBBP5 levels for ERK levels. qPCR-ChIP analysis of H3K4me3 levels were performed on: (B) the positive control, the *RPL41* promoter; and (C) the *FOS* promoter and upstream -3395 negative control region. Samples used for both controls were without EGF treatment. The relative levels are the ratios of immunoprecipitated levels of H3K4me3 to histone H3. Error bars represent standard deviations calculated from three and two biologically independent samples for *FOS* promoter and controls, respectively. Dashed lines and numerical values show the average background values as indicated on the right of each graph and are obtained from ChIP with non-specific α -IgG.

the *RPL41* promoter as a positive control and observed a decrease in H3K4me3 levels at this promoter after RBBP5 depletion (Fig. 6B), consistent with previous results [31]. Next we examined the *FOS* locus and tested both its proximal promoter and a distally located upstream region (centered at -3395 relative to the TSS) of *FOS*. This distal region was used as a negative control region to demonstrate the specificity of the ChIP because the H3K4me3 levels detected at this region were very low (Fig. 6C, right panel) compared to the promoter region (Fig. 6C, left panel). However, we did not see any difference in H3K4me3 levels upon RBBP5 depletion at the *FOS* promoter region either in the basal state or

after 15 min EGF treatment (Fig. 6C). This demonstrates that the changes in unspliced *FOS* transcript levels upon WAR complex depletion are not related to changes in the H3K4me3 levels at its promoter.

Interestingly, we did not see any EGF-mediated increases in H3K4me3 levels in the *FOS* promoter region, consistent with previous results for mouse fibroblasts [32], although in the latter case, changes in methylation were observed in the promoter proximal region of the coding region. Given the lack of effect of RBBP5 depletion, we did not test whether depletion of any of the other subunits had any effect on H3K4me3, as even if they did have an effect, it would not explain the common effect we see on pre-mRNA levels.

DISCUSSION

Previous research suggested that there might be direct interactions between the ERK MAP kinase pathway and the WAR subcomplex. Here, we identified a role for the WAR subcomplex in promoting the efficient processing of nascent transcripts of the IEG *FOS*, providing support for this hypothesis. It is possible that direct interactions occur between these pathways, but we could find no sign of a direct interaction with the ERK pathway as we could find little evidence for phosphorylation of the WAR complex components by ERK (data not shown). Instead our studies imply a more indirect interaction mechanism where the two pathways converge on different steps in the process of IEG activation. The mechanisms underlying the regulation of *FOS* expression are still not completely understood despite extensive studies on this topic [24].

Here we studied the role of the WAR subcomplex in this process and revealed another facet of *FOS* regulation through the control of processing of its primary RNA transcripts. We find that the WAR subcomplex plays a positive role in this process. Importantly, our study also demonstrates the involvement of the WAR subcomplex in gene regulation beyond its well-known role in enhancing the catalytic activity of HMTs, which are associated with depositing H3K4me3 marks at the promoters of active transcribed genes. H3K4me3 was previously shown to be associated with the recruitment of the spliceosomal machinery via interaction with CHD1 and SF3 components [21]. In contrast to that study, we did not uncover a role for H3K4me3 in the processing of *FOS* pre-mRNA, as no change in H3K4me3 level was observed at the *FOS* promoter upon perturbation of the WAR subcomplex. Therefore, the increases in unspliced transcript levels for *FOS* and other IEGs like *ZFP36* that we observed under these conditions appear to occur independently from any activity involving H3K4me3 marks. Nevertheless, we cannot exclude a role for the SET domain-containing proteins acting independently from the WAR subcomplex, even though many studies have shown that SET domain-containing proteins have no or little catalytic activity in H3K4 methylation in the absence of the WAR subcomplex. Besides that, the lack of methylation change suggests a lack of requirement at least for the histone methylating activity of the MLL-WAR complex.

An increase in pre-mRNA could be due to an increase in the transcription rate of *FOS* gene. However, our nuclear run-on assay from RBBP5-depleted cells suggests a positive role in promoting transcription in both basal and induced conditions (data not shown). Knowing that the U2 snRNP-containing SF3 complex is recruited to the chromatin by CHD1 via H3K4me3 recognition [21], we investigated the effects of the WAR complex depletion on regulating mRNA expression of SF3A and SF3B subcomplex of U2 snRNP, as a potential mechanism to explain the splicing defects we observed. However, depletion of the WAR subcomplex had very little effect on the mRNA expression of U2 snRNP subcomplex components (data not shown). Thus, although we can rule out an effect on the expression of some splicing complex components, it is possible that other indirect mechanisms affecting gene expression of other RNA processing factors are operational. However, as we can detect binding of RBBP5 to IEG promoters, this implies at least in part, a direct effect of RBBP5 in regulating these genes.

Overall, we speculate that the WAR subcomplex components could modulate downstream events in RNA synthesis at their target genes by acting independently from SET domain-containing proteins or each might have independent or specific functions, depending on the target. Indeed, independent roles for WAR subcomplex subunits have been demonstrated in several studies. First, *ASH2L* has been shown to act as an oncoprotein and in association with Ha-Ras, it is required for the transformation of rat embryo fibroblasts [15]. This suggests that *ASH2L* alone or an *ASH2L*-containing complex might be involved in events linking to Ras-driven ERK MAPK signaling. In addition, a high expression level of *ASH2L* protein has been shown in hepatocellular carcinoma [33]. A role of *WDR5* in regulating pluripotency and self-renewal of ES cells has recently been reported [34]. Furthermore, RBBP5 has recently been classified as a novel oncogene involved in glioma-genesis. Amplification and overexpression of the *RBBP5* gene were found in patient-derived tumor samples [14]. Although biochemical purification and co-immunoprecipitation studies indicate the presence of the WAR subcomplex [7, 12, 13, 35], compelling evidence for such an independently functioning complex under physiological conditions is still lacking as the experimental conditions may result in the loss of an integral partner of a protein complex.

Overall, our understanding of IEG regulation is mainly based on *FOS*, and detailed descriptions of the regulatory mechanisms for other IEGs such as *ZFP36* and *EGR1* are less abundant [24]. This might be due to the assumption that all IEGs are regulated via the same mechanisms. In addition, recent findings suggest that there are different modes of regulation for IEGs depending on the cell type studied [24]. However, here we provide another example whereby this assumption does not hold true. Although WAR complex depletion leads to increases in pre-mRNA levels of both *FOS* and *ZFP36*, only in the latter case does this translate into increased mature mRNA levels. Thus, although having a common role in pre-mRNA processing, the WAR subcomplex clearly has

different additional regulatory activities towards *FOS* and *ZFP36* regulation. Further study is needed to understand how the changes in *ZFP36* transcript levels are modified, as the increased levels we observed upon WAR complex depletion are apparently not due to an increased transcriptional initiation rate.

In summary, these additional findings further highlight that there is a need to thoroughly investigate all IEGs individually in order to have a comprehensive view of how they are controlled. Ultimately, this might provide clues about how to control their expression in disease states such as cancer.

Acknowledgements. We would like to thank Karren Palmer for technical assistance, Ian Donaldson for bioinformatics analysis, and Shen-Hsi Yang and other laboratory members for their advice and support. We are grateful to Peter Scacheri for providing the RBBP5 ChIP-chip data.

REFERENCES

1. Lee, J-H. and Skalnik, D.G. CpG binding protein (CXXC finger protein 1) is a component of the mammalian Set 1 histone H3-lys4 methyltransferase complex, the analogue of the yeast Set1/COMPASS complex. **J. Biol. Chem.** 280 (2005) 41725–41731.
2. Dou, Y., Milne, T.A., Tackett, A.J., Smith, E.R., Fukuda, A., Wysocka, J., Allis, C.D., Chait, B.T., Hess, J.L. and Roeder, R.G. Physical association and coordinate function of the H3 K4 methyltransferase MLL1 and the H4 K16 acetyltransferase MOF. **Cell** 121 (2005) 873–885.
3. Lee, J.S., Shukla, A., Schneider, J., Swanson, S.K., Washburn, M.P., Florens, L., Bhaumik, S.R. and Shilatifard, A. Histone crosstalk between H2B monoubiquitination and H3 methylation mediated by COMPASS. **Cell** 131 (2007) 1084–1096.
4. Wysocka, J., Swigut, T., Milne, T.A., Dou, Y., Zhang, X., Burlingame, A.L., Roeder, R.G., Brivanlou, A.H. and Allis, C.D. WDR5 associates with histone H3 methylated at K4 and is essential for H3K4 methylation and vertebrate development. **Cell** 17 (2005) 859–872.
5. Yokoyama, A., Wang, Z., Wysocka, J., Sanyal, M., Aufiero, D.J., Kitabayashi, I., Herr, W. and Cleary, M.L. Leukemia proto-oncoprotein MLL forms a SET1-like histone methyltransferase complex with MENIN to regulate Hox gene expression. **Mol. Cell Biol.** 24 (2004) 5639–5649.
6. Issaeva, I., Zonis, Y., Rozavskaja, T., Orlovsky, K., Croce, C.M., Nakamura, T., Mazo, A., Eisenbach, L. and Canaani, E. Knockdown of ALR (MLL2) reveals ALR target genes and leads to alterations in cell adhesion and growth. **Mol. Cell Biol.** 27 (2007) 1889–1903.
7. Patel, A., Vought, V.E., Dharmarajan, V. and Cosgrove, M.S. A novel non-Set domain multi-subunit methyltransferase required for sequential nucleosomal histone H3 methylation by the mixed lineage leukemia protein-1 (MLL1) core complex. **J. Biol. Chem.** 286 (2011) 3359–3360.

8. Hughes, C.M., Rozenblatt-Rosen, O., Milne, T.A., Copeland, T.D., Levine, S.S., Lee, J.C., Hayes, D.N., Shanmugam, K.S., Bhattacharjee, A., Biondi, C.A., Kay, G.F., Hayward, N.K., Hess, J.L. and Meyerson, M. Menin associates with a trithorax family histone methyltransferase complex and with the *hoxc8* locus. **Mol. Cell.** 13 (2004) 587–597.
9. Dou, Y., Milne, T.A., Ruthenburg, A.J., Lee, S., Lee, J.W., Verdine, G.L., Allis, C.D. and Roeder, R.G. Regulation of MLL1 H3K4 methyltransferase activity by its core components. **Nat. Struct. Mol. Biol.** 13 (2006) 713–719.
10. Avdic, V., Zhang, P., Lanouette, S., Groulx, A., Tremblay, V., Brunzelle, J. and Couture, J-F. Structural and biochemical insights into MLL1 core complex assembly. **Structure** 19 (2011) 101–108.
11. Cao, F., Chen, Y., Cierpicki, T., Liu, Y., Basrur, V., Lei, M. and Dou, Y. An Ash2L/RbBP5 heterodimer stimulates the MLL1 methyltransferase activity through coordinated substrate interacts with the MLL1 Set domain. **PLoS One** 5 (2010) e14102. DOI: 10.1371/journal.pone.0014102.
12. Steward, M.M., Lee, J.S., O'Donovan, A., Wyatt, M., Bernstein, B.E. and Shilatifard, A. Molecular regulation of H3K4 trimethylation by ASH2L, a shared subunit of MLL complexes. **Nat. Struct. Mol. Biol.** 13 (2006) 852–854.
13. Patel, A., Dharmarajan, V., Vought, V.E. and Cosgrove, M.S. On the mechanism of multiple lysine methylation by the human mixed lineage leukemia protein-1 (MLL1) core complex. **J. Biol. Chem.** 284 (2009) 24242–24256.
14. Bralten, L.B.C., Kloosterhof, N.K., Gravendeel, L.A.M., Sacchetti, A., Duijm, E.J., Kros, J.M., van den Bent, M.J., Hoogenraad, C.C., Smitt, P.A.E. and French, P.J. Integrated genomic profiling identifies candidate genes implicated in glioma-genesis and a novel LEO1-SLC12A1 fusion gene. **Genes, Chromosomes Cancer** 49 (2010) 509–517.
15. Lüscher-Firzloff, J., Gawlista, I., Vervoorts, J., Kapelle, K., Braunschweig, T., Walsemann, G., Rodgarkia-Schamberger, C., Schuchlantz, H., Dreschers, S., Kremmer, E., Lilischkis, R., Cerni, C., Wellmann, A. and Lüscher, B. The human trithorax protein hASH2 functions as an oncoprotein. **Cancer Res.** 68 (2008) 749–758.
16. Wu, M., Wang, P.F., Lee, J.S., Martin-Brown, S., Florens, L., Washburn, M. and Shilatifard, A. Molecular regulation of H3K4 trimethylation by Wdr82, a component of human Set1/COMPASS. **Mol. Cell. Biol.** 28 (2008) 7337–7344.
17. Wang, P., Lin, C., Smith, E.R., Guo, H., Sanderson, B.W., Wu, M., Gogol, M., Alexander, T., Seidel, C., Weidemann, L.M., Ge, K., Krumlauf, R. and Shilatifard, A. Global analysis of H3K4 methylation defines MLL family member targets and points to a role for MLL1-mediated H3K4 methylation in the regulation of transcriptional initiation by RNA polymerase II. **Mol. Cell. Biol.** 29 (2009) 6074–6085.
18. Mishra, B.P., Ansari, K.I. and Mandal, S.S. Dynamic association of MLL1, H3K4 trimethylation with chromatin and Hox gene expression during the cell cycle. **FEBS J.** 276 (2009) 1629–1640.

19. Ansari, K.I. and Mandal, S.S. Mixed lineage leukemia: roles in gene expression, hormone signaling and mRNA processing. **FEBS J.** 277 (2010) 1790–1804.
20. Bhatt, D.M., Pandya-Jones, A., Tong, A.-J., Barozzi, I., Lissner, M.M., Natoli, G., Black, D.L. and Smale, S.T. Transcript dynamics of proinflammatory genes revealed by sequence analysis of subcellular RNA fractions. **Cell** 150 (2012) 279–290.
21. Sims III, R.J., Millhouse, S., Chen, C.-F., Lewis, B.A., Erdjument-Bromage, H., Tempst, P., Manley, J.L. and Reinberg, D. Recognition of trimethylated histone H3 lysine 4 facilitates the recruitment of transcription postinitiation factors and pre-mRNA splicing. **Mol. Cell** 28 (2007) 665–676.
22. Roberts, P.J. and Der, C.J. Targeting Raf/MEK/ERK mitogen-activated protein kinase cascade for the treatment of cancer. **Oncogene** 29 (2007) 3291–3310.
23. Galbraith, M.D. and Espinosa, J.M. Lessons on transcriptional control from the serum response network. **Curr. Opin. Genet. Dev.** 21 (2011) 160–166.
24. O'Donnell, A., Odrowaz, Z. and Sharrocks, A.D. Immediate-early gene activation by the MAPK pathways: what do and don't we know? **Biochem. Soc. Trans.** 40 (2012) 58–66.
25. Hazzalin, C.A. and Mahadevan, L.C. Dynamic acetylation of all lysine 4-methylated histone H3 in the mouse nucleus: analysis at c-fos and c-jun. **PLoS Biol.** 3 (2005) 2111–2126.
26. Fisher, K., Southall, S.M., Wilson, J.R. and Poulin, G.B. Methylation and demethylation activities of a *C. elegans* MLL-like complex attenuate RAS signaling. **Dev. Biol.** 341 (2010) 142–153.
27. O'Donnell, A., Yang, S.H. and Sharrocks, A.D. MAP kinase-mediated c-fos regulation relies on a histone acetylation relay switch. **Mol. Cell** 29 (2008) 780–785.
28. Marais, A., Ji, Z., Child, E.S., Krause, E., Mann, D.J. and Sharrocks, A.D. Cell cycle-dependent regulation of the forkhead transcription factor FOXK2 by CDK•cyclin complexes. **J. Biol. Chem.** 285 (2010) 35728–35739.
29. Boros, J., Donaldson, I.J., O'Donnell, A., Odrowaz, Z.A., Zeef, L., Lupien, M., Meyer, C.A., Shirley, L.X., Brown, M. and Sharrocks, A.D. Elucidation of the ELK1 target gene network reveals a role in the coordinate regulation of core components of the gene regulation machinery. **Genome Res.** 19 (2009) 1963–1973.
30. Scacheri, P.C., Davis, S., Odom, D.T., Crawford, G.E., Perkins, S., Halawi, M.J., Agarwal, S.K., Marx, S.J., Spiegel, A.M., Meltzer, P.S. and Collins, F.S. Genome-wide analysis of menin binding provides insights into MEN1 tumorigenesis. **PLoS Genet.** 2 (2006) e51. DOI: 10.1371/journal.pgen.0020051.
31. Blobel, G.A., Kadauke, S., Wang, E., Lau, A.W., Zuber, J., Chou, M.M., and Vakoc, C.R. A reconfigured pattern of MLL occupancy within mitotic

- chromatin promotes rapid transcriptional reactivation following mitotic exit. **Mol. Cell** 36 (2009) 970–983.
32. Edmunds, J.W., Mahadevan, L.C. and Clayton, A.L. Dynamic histone H3 methylation during gene induction: HYPB/Setd2 mediates all H3K36 trimethylation. **EMBO J.** 27 (2008) 406–420.
 33. Magerl, C., Ellinger, J., Braunschweig, T., Kremmer, E., Koch, L.K., Höllere, T., Büttner, R., Lüscher, B. and Gütgemann, I. H3K4 dimethylation in hepatocellular carcinoma is rare compared with other hepatobiliary and gastrointestinal carcinomas and correlates with expression of the methylase Ash2 and the demethylase LSD1. **Hum. Pathol.** 41 (2010) 181–189.
 34. Ang, Y-S., Tsai, S-Y., Lee, D-F., Monk, J., Su, J., Ratnakumar, K., Ding, J., Ge, Y., Darr, H., Chang, B., Wang, J., Rendl, M., Bernstein, E., Schaniel, C. and Lemischka, I.R. WDR5 mediates self-renewal and reprogramming via the embryonic stem cell core transcriptional network. **Cell** 145 (2011) 183–197.
 35. Garapaty, S., Xu, C.F., Trojer, P., Mahajan, M.A., Neubert, T.A. and Samuels, H.H. Identification and characterization of a novel nuclear protein complex involved in nuclear hormone receptor-mediated gene regulation. **J. Biol. Chem.** 284 (2009) 7542–7552.